arXiv:1402.0257v1 [astro-ph.SR] 2 Feb 2014

Pulsations and Hydrodynamics of Luminous Blue Variable Stars[1]

J.A. Guzik[a] and C. C. Lovekin[b,c]

ABSTRACT

The Luminous Blue Variable stars exhibit behavior ranging from light curve 'microvariations' on timescales of tens of days, to 'outbursts' accompanied by mass loss of $\sim 10^{-3}$ $M_\odot$ occurring decades apart, to 'giant eruptions' such as seen in Eta Carinae ejecting one or more solar masses and recurring on timescales of centuries. Here we review the work of the Los Alamos group since 1993 to investigate pulsations and instabilities in massive stars using linear pulsation models and non-linear hydrodynamic models. The models predict pulsational variability that may be associated with the microvariations. Using a nonlinear pulsation hydrodynamics code with a time-dependent convection treatment, we show that, in some circumstances, the Eddington limit is exceeded periodically in the pulsation driving region of the stellar envelope, accelerating the outer layers, and perhaps initiating mass loss or LBV outbursts. We discuss how pulsations and mass loss may be responsible for the location of the Humphreys-Davidson Limit in the H-R diagram. The 'giant eruptions', however, must involve much deeper regions in the stellar core to cause such large amounts of mass to be ejected. We review and suggest some possible explanations, including mixing from gravity modes, secular instabilities, the epsilon mechanism, or the SASI instability as proposed for Type II supernovae. We outline future work and required stellar modeling capabilities to investigate these possibilities.

Subject headings: stars: massive – stars: oscillations

1. Introduction

The Luminous Blue Variables (LBVs) are a class of high-mass stars that undergo eruptive events accompanied by mass loss. Many have been discovered in our galaxy, but many are also found in the Large Magellanic Cloud (e.g. Wolf et al. 2000). The LBVs show three different types of variability. In one form, the LBV seems to traverse the H-R diagram at a constant luminosity, but with decreasing effective temperature/increasing radius and increase of 1-2 visual magnitudes during the outburst (Puls 2008). This type of variability is known as S Doradus (SD) variability, and is seen as either a short SD phase, with a timescale less than 10 years, or a long SD phase, with a timescale greater than 20 years.

Another class, or perhaps a separate kind of eruption in the same star, is accompanied by both luminosity and mass increases, with ejection of several solar masses of material, and brightening by 1-3 bolometric magnitudes, and many visual magnitudes. These stars, named the 'supernova impostors' (e.g., Smith et al. 2011; Van Dyk & Matheson 2012), may have recurrences of these 'giant eruptions' on timescales of centuries. In our galaxy, the most well-known examples of the giant eruptions are the LBVs P Cyg and Eta Car. Several candidates have also been detected in the Large Magellanic Cloud (Wolf et al. 2000) and external galaxies (e.g., M33, Clark et al. 2012).

A third kind of variation in the Luminous Blue

[a]Theoretical Design Division, Los Alamos National Laboratory, XTD-NTA, MS T-086, Los Alamos, NM 87545 USA

[b]Theoretical Division, Los Alamos National Laboratory, T-2, MS B-227, Los Alamos, NM 87545 USA

[c]Physics Department, Mount Allison University, Sackville, New Brunswick, Canada

[1]Updated, corrected, and LaTeX typeset version of Guzik & Lovekin (2012) published in Astronomical Review, Vol. 7, p. 3, July 2012.

Variables is the 'microvariations' in luminosity, of a few tenths of a stellar magnitude. These microvariations appear stochastic in nature, but have irregular periods of order of weeks to months (Abolmasov 2011). See also Vink (2012) for a recent review of LBV properties and research questions.

The first and second types of variability recently have been proposed as an explanation for various features seen in supernova (SN) light curves. For example, Kotak & Vink (2006) have proposed that SNe which show quasi-sinusoidal variation in their radio light curve have LBVs undergoing the SD type variations as progenitors. As the mass-loss rates appear to change during a SD outburst (e.g., Stahl et al. 2001, 2003), the resulting circumstellar medium varies in density. LBVs as progenitors of SNe have also been proposed as the progenitors of Type IIn SNe or superluminous SN (e.g. Smith 2010).

The evolutionary status of LBVs is also uncertain. It has long been accepted that massive O stars become LBVs before losing their outer layers to become Wolf-Rayet (WR) stars, and subsequently SN (e.g., Chiosi & Maeder 1986). Stars will lose mass through radiatively driven winds throughout these phases, and it has been shown that some LBV envelopes have enriched He abundances and evidence of CNO-cycle processing indicating that outer layers have been removed to expose material that had previously experienced hydrogen burning (Najarro et al. 1997; Najarro 2001). However, with recent downward revisions of theoretical mass-loss rates, it seems that radiatively driven mass loss cannot remove enough material to match the observed masses of WR stars (about 20 $M_{\odot}$). If most or all massive stars end as WR stars, the most massive stars may need a series of giant eruption events during an LBV phase to reach the masses of typical WR stars (Smith et al. 2006).

The LBVs are cooler than the core He-burning WR stars, which have been stripped of their outer layers, presumably during an earlier LBV phase. The most luminous LBVs are hotter and brighter than the Humphreys-Davidson Limit (H-D Limit, Humphreys & Davidson 1994) in the H-R diagram (see Fig. 1), and may be on their first crossing of the H-R diagram in a shell H-burning or core He-burning phase. At lower initial masses and luminosities, stars are found below the Humphreys-Davidson limit and across the width of the H-R diagram as blue, yellow, and red supergiants. At present, the physical origin of the Humphreys-Davidson limit is not understood, and the highest initial mass which can evolve to the red supergiant region is determined observationally.

While much analytical work, atmosphere and wind modeling, and observational work has been assembled to understand and categorize LBV phenomena, and some explanations of the origin of LBV winds and outbursts have been proposed, to our knowledge very little research has been published in the refereed literature on the role of stellar pulsations in producing LBV microvariations or initiating outbursts or winds. In addition, a pulsational instability or some other hydrodynamic instability deep in the core must be responsible for initiating LBV giant eruptions.

Here we review the work of the group at Los Alamos National Laboratory from 1993 to the present that has before only been summarized briefly in abstracts or published in conference proceedings.[2] (These conference presentations are designated by asterisks in the References.) We focus on linear stellar pulsation modeling using 1-D stellar evolution models including mass loss, and 1-D nonlinear hydrodynamic envelope models using the Dynstar Lagrangian stellar pulsation hydrodynamics code (Ostlie 1982, 1990; Cox 1983, 1990; Cox & Ostlie 1993) which includes a time-dependent convection treatment. We also suggest some possible mechanisms for initiating LBV giant eruptions. We hope that this review will motivate work by those who have more advanced computational tools to further investigate instabilities that may be responsible for LBV episodic mass loss and giant eruptions.

For a recent comprehensive overview of the properties of Eta Car and other known LBV stars, we recommend the review articles in the volume edited by Davidson and Humphreys, Eta Carinae and the Supernova Impostors, vol. 384 of the Springer Astrophysics and Space Science Library published in 2012.

[2]Since the original publication of this paper, work in this area by Lovekin & Guzik has been submitted for publication in MNRAS.

2. Pulsations and LBV Outbursts

To investigate LBV models, we began in the mid 1990s by evolving some high-mass models using an updated version of the Iben (1963, 1965a,b) stellar evolution code including mass loss (Brunish & Truran 1982a,b). The code included the analytical Stellingwerf (1975a,b) fit to the Cox-Tabor opacity tables that was adjusted to roughly calibrate the opacities to Lawrence Livermore OPAL opacities (Iglesias & Rogers 1996). These new higher opacities had recently been shown to explain many problems in stellar modeling, including the Cepheid mass problem, and the cause of β Cep star pulsations (Rogers & Iglesias 1994). We evolved 50 $M_\odot$ and 80 $M_\odot$ models using the parameterized mass-loss formula of Nieuwenhuijzen & de Jager (1990) intended to generally fit observed mass-loss rates across the upper H-R diagram. We adjusted this prescription to increase the mass loss more rapidly with increasing radius, as we wanted to develop models that had a variety of envelope helium abundance enrichments when they arrived in the LBV instability region on their first crossing of the H-R diagram. Figure 1 shows our evolution tracks for 50 and 80 $M_\odot$ models with metallicitiy Z=0.02, appropriate for galactic LBVs. The two crosses show the endpoints of an 80 $M_\odot$ evolution sequence at Z = 0.01, a metallicity chosen to approximate the lower metallicity of the Large Magellanic Cloud where many LBV stars are found. Figure 2 shows the endpoints of the evolution tracks on the H-R diagram of Humphreys & Davidson (1994) in relation to many well-known LBV stars and the H-D limit.

We then tested these models for pulsational instabilities using a linear nonadiabatic code developed by Pesnell (1990). The models show that pulsations (both radial and nonradial) are driven by the 'kappa-gamma' mechanism (see, e.g., J.P. Cox 1980) due to ionization of Fe-group elements in the stellar envelope at ∼200,000 K. The modes are highly nonadiabatic because of the low density and high luminosity of these stars, and the periods can be radically different and even not able to be associated with the corresponding modes found in an adiabatic analysis, motivating them to be called 'strange modes' in the literature (see, e.g., Glatzel et al. 1999; Glatzel 1999, 1994; Glatzel & Mehren 1996). The predicted linear growth rates of strange modes are as large as several hundred percent/period, much higher than the 0.001/period typical of most pulsating variables of lower mass. Low-mass evolved stars, such as Miras, are also known to have large growth rates (e.g., Cox & Ostlie 1993).

We then used the nonlinear hydrodynamics code Dynstar (Ostlie 1982, 1990; Cox 1983; Cox & Ostlie 1993) to examine the nonlinear hydrodynamic behavior of these models. The Dynstar code was updated to include the same Stellingwerf opacity fit adjusted to the OPAL opacities used in the evolution modeling. In the hydro code, we construct envelope-only models with 60-120 zones distributed from above the photosphere down to a few million K. The envelopes of these stars are very tenuous, so our LBV models include 95% of the star's radius, but only 0.2% of the mass! Table 1 summarizes the linear pulsation model results for the models that were used as input for the hydrodynamic analysis. We initiated the pulsations with radial velocity amplitude 1 km/sec outward in the radial mode (Fundamental, 1st Harmonic, or 2nd Harmonic) that we found to be most unstable from the linear analysis (when practical).

The unique feature of the Dynstar code that proved essential to explaining the behavior of the models is a time-dependent treatment of convection. This treatment is a modification of mixing-length theory (Böhm-Vitense 1958) and allows for the lag in adjustment of the convective flux that is changing dynamically with the pulsation. Spatial averaging over a few zones allows for convective effects to communicate with nearby zones. The time-dependent convection treatment is described in more detail in Section 2.2 below.

We found in our initial nonlinear study that the pulsation amplitudes are regulated by metallicity and by the envelope helium (Y) abundance (Guzik et al. 1996, 1999b, 2004). Figures 3, 4, 5, and 6 show photospheric radial velocities vs. time, with negative velocities indicating outward flows. If the He abundance is sufficiently low (the exact value depends on mass and metallicity; see Table 2), the models quickly develop a large outward photospheric velocity. Layers just below the photosphere continue to pulsate, producing shocks or waves. These can interact with the photospheric

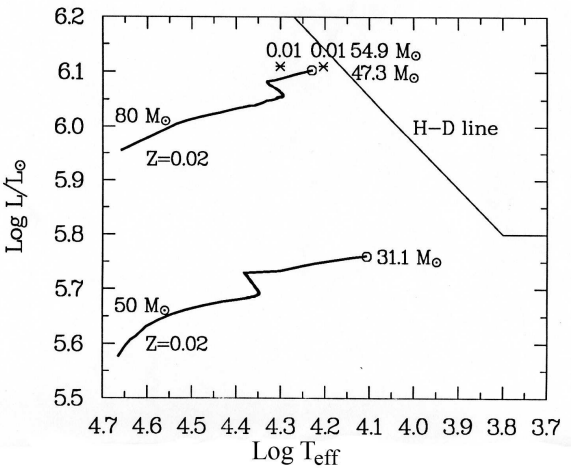

Fig. 1.— Evolution tracks and final masses after mass loss for models of initial mass 80 and 50 $M_\odot$ that were analyzed for stellar pulsations (endpoint circles and crosses.) The models lie in the region of the H-R diagram where LBV instabilities originate, to the left of the Humphreys-Davidson limit. The final mass of the Z=0.01 model (after mass loss) is 54.9 $M_\odot$.

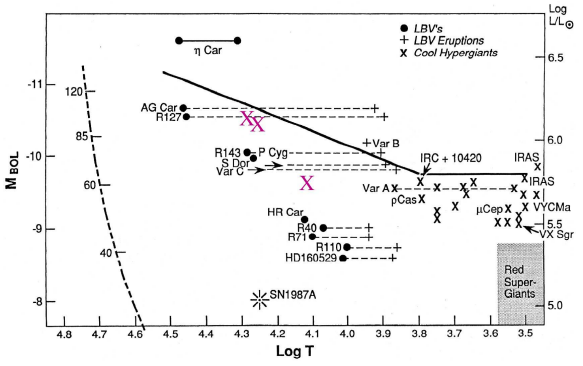

Fig. 2.— Location of models (Red Xs) on H-R diagram from (Humphreys & Davidson 1994).

layers to produce an abrupt outward increase in velocity. The photosphere attempts to recover, but because the hydro code cannot follow mass outflows, and the opacity and equation-of-state (EOS) tables and radiative transfer models are no longer appropriate for the outermost layers well beyond the photosphere, the model cannot be continued further in time. The final radial velocities we find (about 250 km/sec) are still lower than the escape velocity for a non-rotating model ($v_{esc} \sim$ 370 km/sec). We associate these abrupt increases in radial velocity with the initiation of an "outburst".

The increase in envelope He abundance has a stabilizing effect on the models; as the envelope He abundance increases, the outbursts disappear, to be replaced by regular pulsations. If the He abundance of the model is decreased further, the amplitude of the pulsation decreases. These results are summarized in Table 2, which shows the exact He and metallicity (Z) dependence for each model.

2.1. The Eddington Limit

An important characteristic that determines whether models "outburst" (i.e., exhibit an abrupt increase in photospheric radial velocity from which it is difficult to recover) appears to be whether the local radiative luminosity of layers with temperatures greater than 100,000 K exceeds the Eddington Luminosity limit at some point during the pulsation cycle. The Eddington Luminosity is defined as

$$L_{Edd} = \frac{4\pi GMc}{\kappa} \qquad (1)$$

where G is Newton's gravitational constant, M is the stellar mass, c is the speed of light, and κ is the radiative opacity. When this luminosity is reached, the outward force due to radiation pressure exceeds the force due to gravity. In a non-pulsating model in hydrostatic equilibrium, if the opacity becomes too high, blocking the emerging radiation, convection turns on to transport the luminosity, so the model stays in hydrostatic equilibrium and avoids exceeding the Eddington limit. If, in a pulsating model, the convection is allowed to adapt instantaneously, convection will also turn on and prevent the local radiative luminosity from ever exceeding the Eddington lumi-

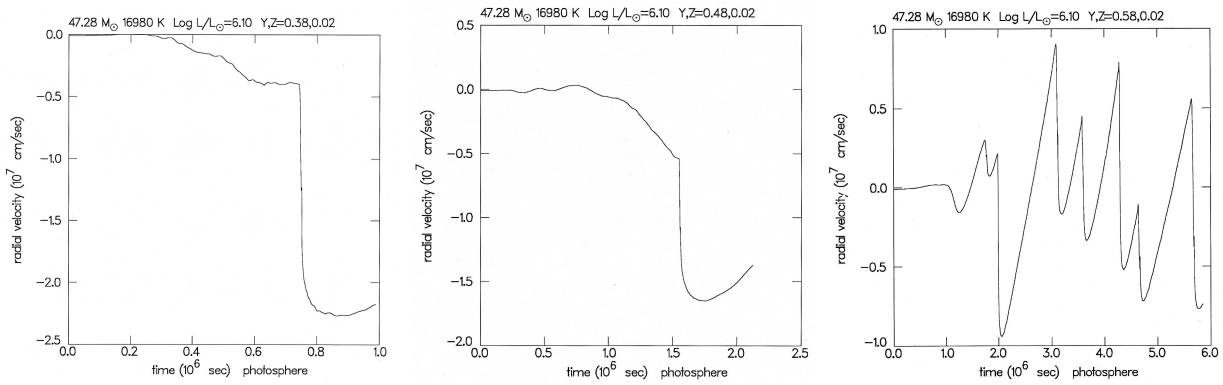
47.28 M⊙ 16980 K Log L/L⊙=6.10 Y,Z=0.38,0.02
47.28 M⊙ 16980 K Log L/L⊙=6.10 Y,Z=0.48,0.02
47.28 M⊙ 16980 K Log L/L⊙=6.10 Y,Z=0.58,0.02
radial velocity (10^7 cm/sec)
time (10^6 sec) photosphere

Fig. 3.— Photospheric radial velocity vs. time for envelope models with helium mass fraction Y=0.38 (left), 0.48 (center), and 0.58 (right) and Z=0.02. Negative radial velocity is outward flow. The Y=0.38 and 0.48 models show large abrupt increase in outward radial velocity. For comparison, the escape velocity for a non-rotating model is 370 km/sec (3.7×10^7 cm/sec). An increase in Y abundance (to 0.58) stabilizes "outburst" behavior.

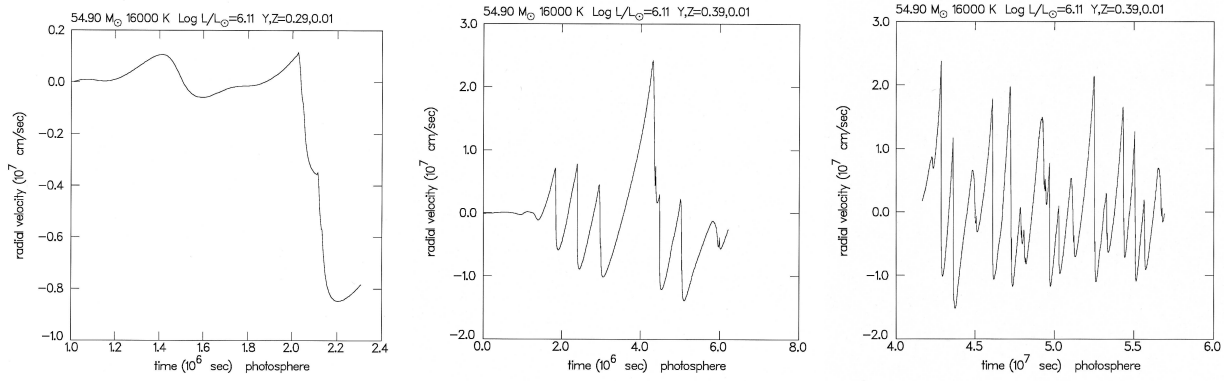
54.90 M⊙ 16000 K Log L/L⊙=6.11 Y,Z=0.29,0.01
54.90 M⊙ 16000 K Log L/L⊙=6.11 Y,Z=0.39,0.01
54.90 M⊙ 16000 K Log L/L⊙=6.11 Y,Z=0.39,0.01
radial velocity (10^7 cm/sec)
time (10^6 sec) photosphere
time (10^7 sec) photosphere

Fig. 4.— Photospheric radial velocity vs. time for envelope models with Y=0.29 and Y=0.39, and Z=0.01. For Y=0.29, this lower Z=0.01 model (left) shows a large abrupt increase in radial velocity. For comparison, escape velocity for a non-rotating model is 380 km/sec (3.7×10^7 cm/sec). For Y=0.39 (center), the model shows steady multimode pulsations. The model is continued to a later time (right) where the pulsations are still evident.

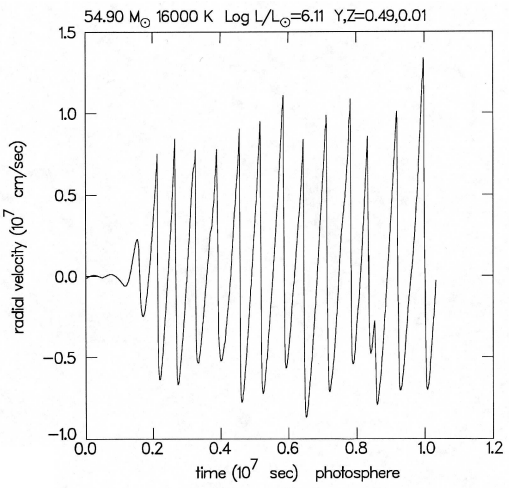

Fig. 5.— Photospheric radial velocity vs. time for envelope model with Y=0.49 and Z=0.01. The model shows steady multimode pulsations at lower amplitude than for Y=0.39 models, and period of about 7.6 days.

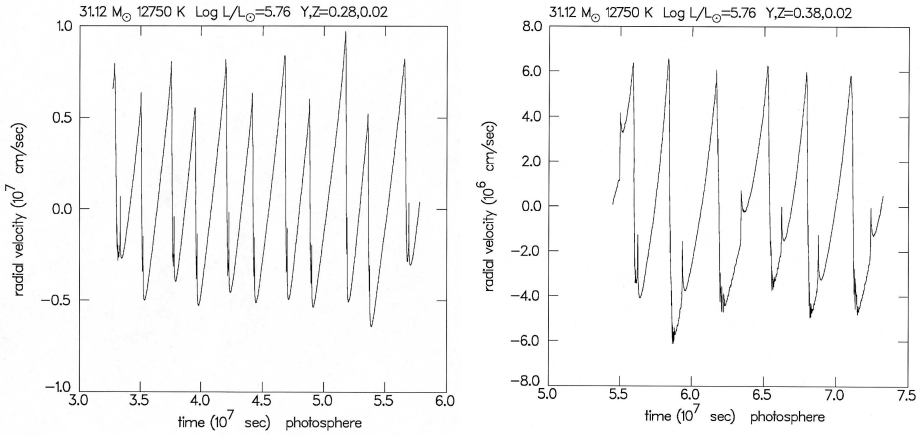
31.12 M⊙ 12750 K Log L/L⊙=5.76 Y,Z=0.28,0.02
radial velocity (10^7 cm/sec)
time (10^7 sec) photosphere
31.12 M⊙ 12750 K Log L/L⊙=5.76 Y,Z=0.38,0.02
radial velocity (10^6 cm/sec)
time (10^7 sec) photosphere

Fig. 6.— Photospheric radial velocity vs. time for envelope models with Y=0.28 and 0.38 and Z=0.02. These lower mass and luminosity models exhibit steady pulsations with periods ∼26 d for the Y=0.28 model, and ∼35 d for the Y=0.38 model. For comparison, the escape velocity for a non-rotating model is 280 km/sec. (2.8×10^7 cm/sec)

Table 1: Linear pulsation model results for models analysed hydrodynamically.

47.28 $M_\odot$ T_{eff} = 16980 K, Z=0.02
High-mass Galactic LBV near H-D Limit

Envelope Y abundance	Linear Period (days)	Growth rate/ period
0.38	9.5	0.70
	8.6	6.0[a] (2H)
	4.4	1.3
0.48	10.6	0.40[a] (F)
	33.3	1.1
0.58	15.1	2.3[a] (F)
	12.2	0.80
	7.1	2.2

54.9 $M_\odot$ T_{eff} = 16000 K, Z=0.01
High-mass LMC LBV near H-D Limit

Envelope Y abundance	Linear Period (days)	Growth rate/ period
0.29	18.0	0.40 (F)
0.39	17.6	0.43[a] (1H)
	33.3	3.6
0.49	28.8	1.4 (F)

31.1 $M_\odot$ T_{eff} = 12750 K, Z=0.02
Lower-mass LBV below horizontal part of H-D Limit

Envelope Y abundance	Linear Period (days)	Growth rate/ period
0.28	22.4	0.96 (F)
0.38	23.0	0.80 (F)

[a]Mode used for hydrodynamic analysis

nosity. However, in the more realistic pulsating model with time-dependent convection, the convection takes some time to turn on during a pulsation cycle, so the Eddington limit can be periodically exceeded. *Including the time dependence of convection is therefore the key to causing the pulsation driving layers to exceed the Eddington limit and initiate outbursts.*

The nonlinear pulsation results are summarized in Table 2. For each model, we list whether the model showed an outburst. If no outburst was present, the maximum velocity is given instead (column 3). The period of the resulting pulsation (if applicable) is given in column 4. In column 2, we state whether there were optically thick zones which exceeded the Eddington limit for part of the pulsation cycle. Outbursts are only triggered if the luminosity exceeds the Eddington luminosity in the driving region, where the temperature is 100,000-200,000 K. As a result of the delay in the onset of convection, there is a buildup of radiation pressure, which gives a push to the layers above. Figures 7 and 8 show the Eddington luminosity, convective luminosity and radiative luminosity in the driving region of models of 47 and 31 $M_\odot$ respectively. The local radiative luminosity periodically exceeds the Eddington luminosity, before dropping sharply when convection turns on. If there is enough mass in the layers above the region exceeding the Eddington limit, this may result in an outburst. In many of the models, in the surface zones (near and above the photosphere), the Eddington luminosity is exceeded for at least part of the time, but there is not enough mass in and above these zones to drive an outburst.

2.2. Time dependent convection treatment

The treatment of time-dependent convection used in Dynstar is that outlined by Ostlie (1990) (see also Cox 1990). The treatment is a modification of the Böhm-Vitense (1958) mixing-length theory. In this model, the mixing length is the distance a convective eddy can travel before reaching equilibrium with the surrounding medium. In a static model envelope, the luminosity carried by this convection is given by

$$L_{conv} = 4\pi r^2 \frac{4T\rho C_p}{g\ell Q} v_c^{o3} \qquad (2)$$

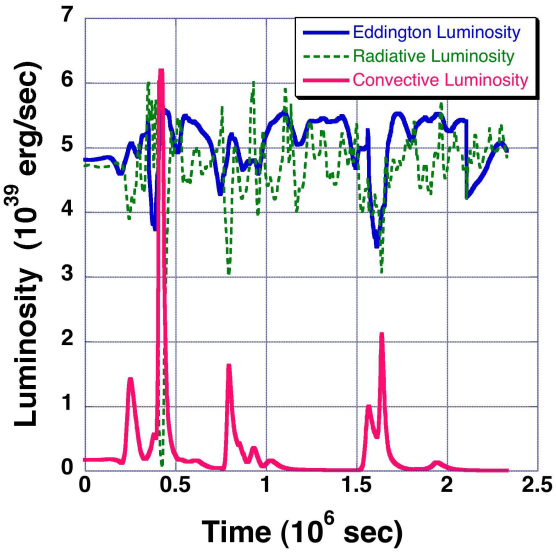

Fig. 7.— Eddington, radiative, and convective luminosity of 47 $M_\odot$ model with T_{eff} = 16,980 K in the driving region of the 60 zone envelope model (T >100,000 K). The radiative luminosity (green) sometimes exceeds the Eddington Limit (blue), until the amount of luminosity carried by convection (red) increases later to transport the excess.

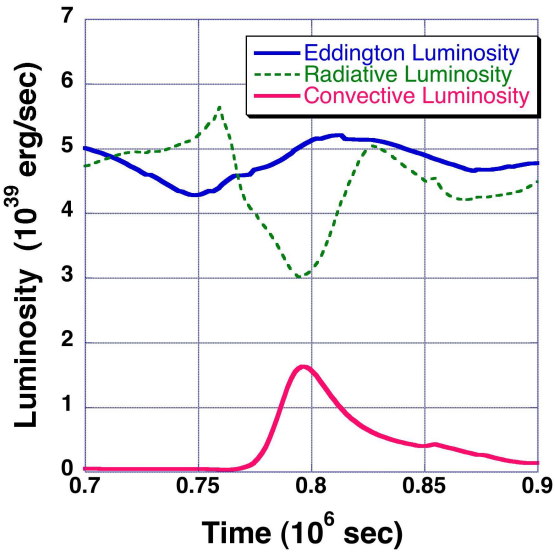

Fig. 8.— Same as Figure 7, but zooming in on a small time region, where it is clear that the radiative luminosity (green) exceeds the Eddington limit (blue) before convection can turn on to transport the luminosity (red).

Table 2: Summary of nonlinear pulsation results.

47.28 $M_\odot$ 16980 K, Z=0.02

Y	Optically Thick Zones with $L_{rad} > L_{Edd}$	Outcome	Period (days)
0.38	Yes	"Outburst"	n/a
0.48	Yes	"Outburst"	n/a
0.58	Yes	V_{max} 100 km/s	∼4.6

54.9 $M_\odot$ 16000 K, Z=0.01

Y	Optically Thick Zones with $L_{rad} > L_{Edd}$	Outcome	Period (days)
0.29	Yes	"Outburst"	n/a
0.39	None	V_{max} 200 km/sec	∼10.5
0.49	None	V_{max} 100 km/sec	7.6

31.1 $M_\odot$ 12750 K, Z=0.02

Y	Optically Thick Zones with $L_{rad} > L_{Edd}$	Outcome	Period (days)
0.28	None	V_{max} 90 km/sec	26
0.38	None	V_{max} 60 km/sec	35

where r, T, p, ρ, C_p and g are the local radius, temperature, pressure, density, specific heat and gravity respectively. The convective velocity, v_c^o is given by

$$v_c^o = \frac{1}{r\sqrt{2}} \frac{g^{1/2} Q^{1/2} \ell}{H_p^{1/2}} f \tag{3}$$

where the mixing length, ℓ, is a variable parameter, typically of order 1. The pressure scale height, H_p is defined to be $P/\rho g$. The parameter Q is the logarithmic density gradient

$$Q = \left(-\frac{\partial log\rho}{\partial T} \right)_P \tag{4}$$

which is exactly 1 for an ideal gas with constant mean molecular weight.

The convective velocity, v_c^o is for the static case, where the parameter f is defined as

$$f = \left[\sqrt{1 + 4A^2(\nabla - \nabla_{ad})} - 1 \right] / A \tag{5}$$

where

$$\nabla = \frac{dlogT}{dlogP} \tag{6}$$

and

$$A \equiv \frac{Q^{1/2} C_p \kappa g \rho^{5/2} \ell^2}{12\sqrt{2} acP^{1/2} T^3}. \tag{7}$$

$\nabla - \nabla_{ad}$ is the superadiabatic gradient, κ is the local opacity of the material, and a is the radiation constant.

To modify this theory to include time-dependent convection, the convective eddy velocity (and hence the convective luminosity) should respond to changes in the local conditions, but not instantaneously. The convective eddy velocity is also dependent on effects from neighboring zones.

First, we account for the time dependence of the convective velocity, using a quadratic Lagrange interpolation, as illustrated in Fig. 9. This interpolation uses the previous two time steps and the instantaneous value (from the original mixing length theory) to determine the current convective velocity:

$$\begin{aligned} v_{c,i}^n = & \frac{(t' - t_{n-1})(t' - t_{n-2})}{(t_n - t_{n-1})(t_n - t_{n-2})} v_{c,i}^o \\ & + \frac{(t' - t_n)(t' - t_{n-2})}{(t_{n-1} - t_n)(t_{n-1} - t_{n-2})} v_{c,i}^{n-1} \\ & + \frac{(t' - t_n)(t' - t_{n-1})}{(t_{n-2} - t_n)(t_{n-2} - t_{n-1})} v_{c,i}^{n-2} \end{aligned} \tag{8}$$

where

$$t' \equiv t_{n-1} + \tau(t_n - t_{n-1}) \tag{9}$$

and

$$\tau \equiv \frac{v_{c,i}^n (t_n - t_{n-1})}{\ell} l_{fac} \tag{10}$$

for $0 \leq \tau \leq 1$ and $l_{fac} \sim 1$.

The quantity l_{fac} is the fraction of a mixing length the convective eddy can travel in one time step. The t' incorporates a phase lag, so there can be some delay before the convective flow begins.

The convective velocity can also depend on nonlocal effects, and so this treatment includes a spatial average over neighboring zones. Zones within one mixing length are assumed to have some contribution to the local conditions. Incorporating all of these, the convective velocity for zone i at time step n is

$$\begin{aligned} \overline{v}_{c,i}^n = & a_{i-1} v_{c,i-1}^{n-1} + a_{i+1} v_{c,i+1}^{n-1} \\ & + (1 - a_{i-1} - a_{i+1}) v_{c,i}^n \end{aligned} \tag{11}$$

where $v_{c,i}^n$ is the convective velocity from the time averaging for the current time step (n) and zone (i). The weighting factor a for zone k is given by

$$a_k = a_{fac} \left(1 - \frac{|r_k - r_i|}{\ell} \right) \tag{12}$$

where a_k constrained to be between 0 and an averaging factor, a_{fac}, and $a_{fac} \leq 1/3$ is a free parameter. This final form of the convective velocity is then used in the first equation to calculate the time-dependent convective luminosity.

2.3. An explanation for the H-D limit?

For high-mass models near the H-D limit, pulsations in our models grow to large amplitudes (>100 km/sec). The pulsation periods and amplitudes we find are similar to those of observed LBV microvariations, which are typically between 5 and 50 days, with amplitudes of ∼0.1 magnitude or less (see, e.g., van Genderen et al. 1985, 1990).

When the deeper (adiabatic) regions of the envelope exceed L_{Edd}, an "outburst" occurs. The radial velocity at the photosphere remains negative, and the radii of outer zones monotonically

increase during several pulsation cycles. An increase in envelope helium abundance lowers the opacity in driving regions and appears capable of limiting the pulsation amplitudes and putting an end to the "outbursts".

These nonlinear hydro model investigations motivate the following picture for the reason for the H-D limit in the H-R diagram: Stars of initial mass >50 $M_\odot$ repeatedly outburst and lose mass until their envelopes are enriched in helium and outbursts are stabilized. These stars never evolve past the H-D line. Pulsation-driven winds with a high mass-loss rate keep these stars to the blue of H-D line (e.g., S Dor, AG Car).

Stars of initial mass <50 $M_\odot$ pulsate on first crossing of H-R diagram, but do not outburst. These stars are able to evolve to become yellow and red supergiants. After they have lost considerably more mass as RSGs and evolve back to the blue, their increased L/Mratio may cause them to exceed the Eddington limit and experience outbursts (e.g., HR Car, R40, R71).

In fact, LBVs have been shown to be enriched with He (Najarro et al. 1997), with Y as high as 0.6. The effects of this He enrichment on mass-loss rates have been studied by Vink & de Koter (2002), with more helium resulting in higher mass-loss rates at high temperatures, and lower mass-loss rates at low temperatures. The pulsational stability of massive stars has been studied by Shiode et al. (2012), but only in terms of metallicity, not helium composition. Clearly, there is still both theoretical and observational work to be done in this area to confirm the effects of composition on pulsational stability and outbursts of LBVs.

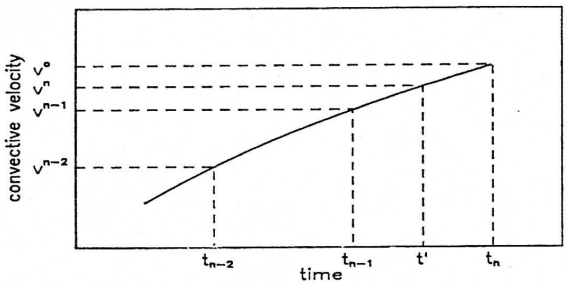

Fig. 9.— The time dependence of the convective velocity. A three-point Lagrange interpolation polynomial is used to find the time-modulated convective velocity. Figure from Ostlie (1990).

2.4. Winds or eruptions?

Since the envelopes of LBVs are very tenuous, we have shown only in our hydro models that this mechanism can trigger an instability and accelerate shells of 10^{-4} solar masses (the mass of the envelope). We have not modeled the outflow or winds or recovery from a mass-loss episode. Perhaps pulsation initiates the flow, and shocks and line-driven winds accelerate it. Our models may explain pulsation-driven mass loss, or irregular mass-loss rates, modulated by the buildup of pulsation amplitude. More work is required to follow a mass loss episode and recovery, to determine whether this mechanism could be responsible for the LBV outbursts.

3. Hydrodynamics of blue stars of lower initial mass

Our initial evolution and hydrodynamic models used the Stellingwerf analytical fit to Cox-Tabor opacity tables, augmented by roughly a factor of two to account for increased opacities in newer tables. In ∼1997 we implemented interpolations on the OPAL (Iglesias & Rogers 1996) opacities, supplemented for layers above the photosphere by the Alexander & Ferguson (1994, 1995) tables. The increased opacities, combined with interpolation in tables caused the hydrodynamic behavior to become more ragged and less stable. We were also unable to evolve very massive stars with high luminosity/mass ratio (M >80 $M_\odot$) including mass loss as the static models were already exceeding the Eddington limit in their outer layers and were not in hydrostatic equilibrium. To study the hydrodynamic behavior in a more stable regime and facilitate parameter studies, we decided to investigate models of about 20 $M_\odot$ near the top of the β Cephei instability strip on the main sequence (see also Guzik & Austin 2005). Note that some comparable nonlinear hydrodynamic calculations were carried out by Dorfi & Gautschy (2000) for a 30 $M_\odot$ model.

The opacity of elements near Fe (atomic number Z∼26) was found to be important for solving the Cepheid mass problem (Rogers & Iglesias 1994), and also to explain the pulsations of two

classes of nonradially pulsating main-sequence stars, the slowly pulsating B (SPB) stars and the β Cephei stars (Pamyatnykh 2002). The β Cephei and SPB stars are burning hydrogen in their core, and are in the main-sequence phase of stellar evolution. SPB and β Cephei stars pulsate in both radial and nonradial low-amplitude pulsations. The modulation of radiation due to ionization of Fe-group elements (Fe, Co, Ni) at temperatures in the envelope around 200,000 K can explain the pulsation driving. As these stars evolve, they exhaust central hydrogen in their convective core, the core collapses, and the star begins burning hydrogen in a shell (after the 'blue hook' on the H-R diagram). The envelope subsequently expands and the stars become more susceptible to higher amplitude radial pulsation since the envelope is less tightly bound.

The kappa (κ) or more correctly, "kappa-gamma" effect is due to the modulated blocking and releasing of radiation during a pulsation cycle by increasing opacity in ionizing regions (see, e.g., J.P. Cox 1980). This modulation allows work to be put into increasing the amplitude of a perturbation, until enough energy begins to be dissipated again at some limiting amplitude. If extra energy is blocked in a layer when the star is smallest (layer is compressed), then it will increase the pressure and give an extra boost to expansion. If the energy is then released when the star is largest (layer is expanded), this lowers the pressure and removes some support against gravity, so that the layer overshoots its equilibrium radius at compression.

For a mode to be pulsationally unstable, the integrated driving throughout all layers must exceed the radiative damping. Regions that produce pulsating driving by the κ effect are where the opacity increases with increasing temperature, as it does in ionizing regions. Stars are known to pulsate due to the ionization of hydrogen (e.g. Mira red giant variables, DA white dwarfs), helium (e.g. Cepheids, δ Scuti stars, DB white dwarfs), and iron (e.g. β Cephei and Slowly Pulsating B stars). See Aerts, Christensen-Dalsgaard & Kurtz (2010) for a recent volume on pulsating variable stars.

Figure 10 shows our evolution track calculated with the Iben code for composition X, Y, Z = 0.70, 0.28, 0.02 using the Grevesse & Noels (1993) solar element mixture superimposed on the H-R diagram of Pamyatnykh (2002). The green X marks the location of the T_{eff}~22,000 K models for which we studied the pulsational stability. For a 20 $M_\odot$ model, the radius increases from 6 $R_\odot$ on the zero-age main sequence to 15 $R_\odot$ before the 'blue hook' at the end of the main sequence, and then to 23 $R_\odot$ after the 'blue hook'. Our linear pulsation analysis used a model-building code described by Cox (1983) that was updated to include the OPAL opacities, and the Pesnell (1990) nonadiabatic pulsation code with 500 zones, and we used the Dynstar code for the 60-zone envelope hydrodynamic models.

To investigate the effects of composition and temperature more systematically, we first examined the driving region using linear models, where we could vary one parameter at a time (Y, Z, T_{eff}). Figures 11-14 show the results of these tests.

In Figures 11-13, we have only studied envelope models in which we artificially vary Y, T_{eff}, and Z. These models were made by evolving a model to a given point with one set of parameters, and then artificially holding all but one of the parameters constant while varying the last one. For example, the different models in Figure 11 were made by holding radius, luminosity and temperature constant while varying the He abundance (Y). However, when models are evolved from the ZAMS with the changed He abundance, the luminosity, radius, and envelope structure change relative to the original model. In this case, the structure changes such that pulsation driving decreases with increasing He abundance (Figure 14).

Tables 3 and 4 summarize the linear pulsation behavior of the models used in the parameter study in Figures 11-13, and for the evolved models shown in Figure 14.

Next we show a series of plots (Figures 15-21) of the behavior of these models in the nonlinear hydrodynamics code. Models are initiated in the radial fundamental mode with radial velocity amplitude 5 km/sec.

The abundance of Fe and He in stellar envelopes is predicted to affect the pulsational instability and amplitudes of 20 $M_\odot$ models with photospheric temperatures near 22,000 K at the edge of the β Cep instability strip. The pulsations are driven by the κ effect in the region of ionization of Fe-group elements near 200,000 K. In our models, the pulsation driving and amplitude

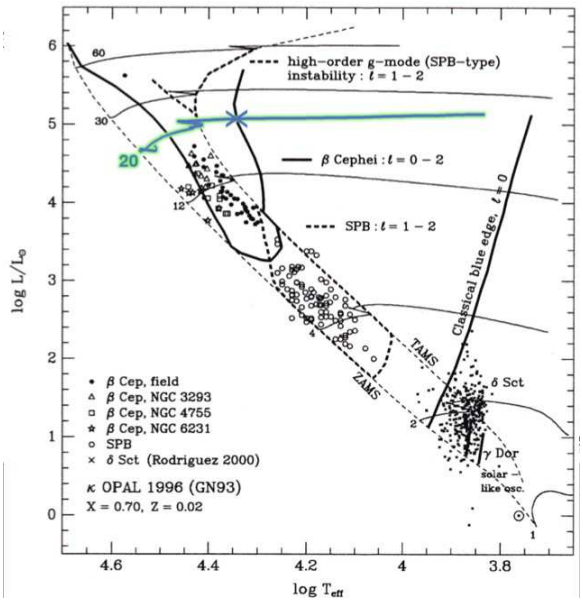

Fig. 10.— H-R diagram showing the main-sequence variables (from Pamyatnykh 2002). The green evolution track is our 20 $M_\odot$ model superimposed. The green cross marks the position where we tested our model for pulsations.

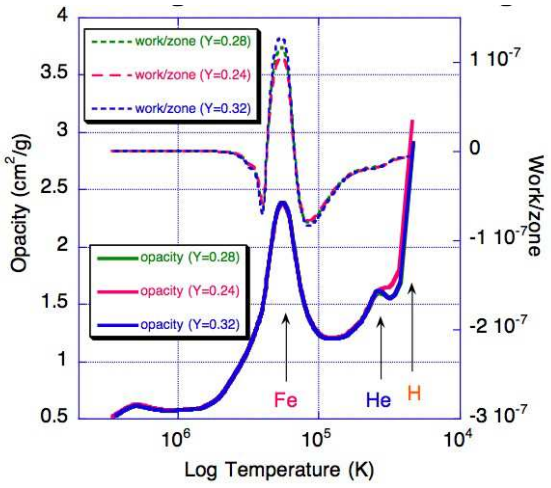

Fig. 11.— Opacity and work per zone for nominal 20 $M_\odot$ model with T_{eff} = 22,000 K in which we varied the envelope Y abundance. For fixed effective temperature, radius (∼23 $R_\odot$), and luminosity, the pulsation driving increases with increasing Y.

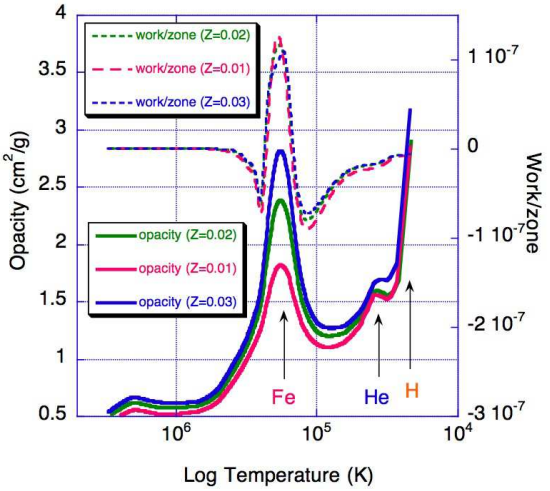

Fig. 12.— For fixed effective temperature, radius (∼23 $R_\odot$), luminosity, and Y abundance, the pulsation driving increases with increasing Z.

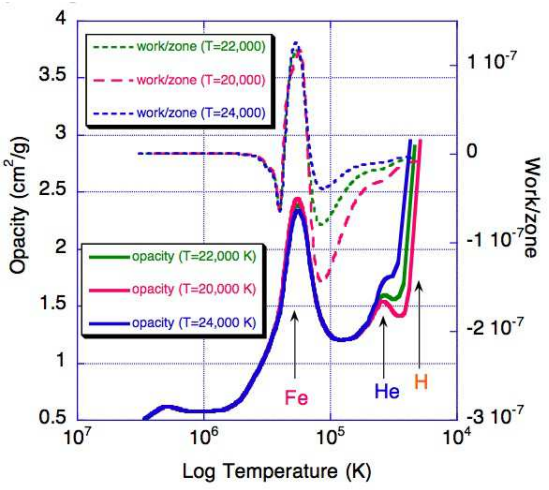

Fig. 13.— For fixed composition and luminosity, linear growth rate increases for higher T_{eff} (younger) models.

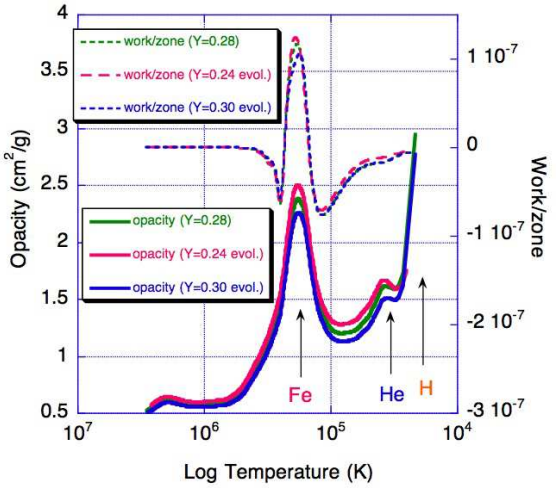

Fig. 14.— Linear pulsation behavior of evolved 20 $M_\odot$ models with varying initial Y and with T_{eff} = 22,139 K.

Table 3: Parameter study for linear pulsations of models, varying Y, Z, and T_{eff}.

Y, Z	T_{eff} (K)	Fund. mode period (days)	Growth rate/ period (+≡unstable)
0.24, 0.02	22,000	0.888	-0.0318
0.28, 0.02	22,000	0.877	-0.0236
0.32, 0.02	22,000	0.868	-0.0160
0.28, 0.01	22,000	0.833	-0.0556
0.28, 0.02	22,000	0.877	-0.0236
0.28, 0.03	22,000	0.916	+0.0186
0.28, 0.02	24,000	0.644	+0.0374
0.28, 0.02	22,000	0.877	-0.0236
0.28, 0.02	20,000	1.227	-0.1028

Table 4: Linear pulsation behavior of 20 $M_\odot$ evolved models with T_{eff} = 22,139 K.

Y, Z	T_{eff} (K)	Fund. mode period (days)	Growth rate/ period (+≡unstable)
0.24, 0.02	98,988	0.756	-0.0166
0.28, 0.02	111,370	0.858	-0.0189
0.30, 0.02	125,015	0.980	-0.0223

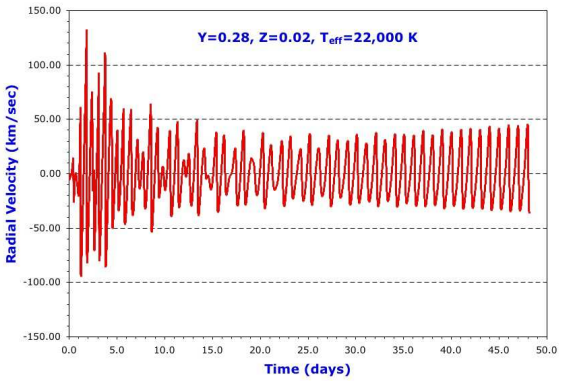

Fig. 15.— Radial velocity of the photosphere vs. time for evolved 20 $M_\odot$ model with Y=0.28, Z=0.02. The amplitude rapidly increases and then decreases as the preferred period appears to be longer than the initial one, with slow amplitude growth thereafter.

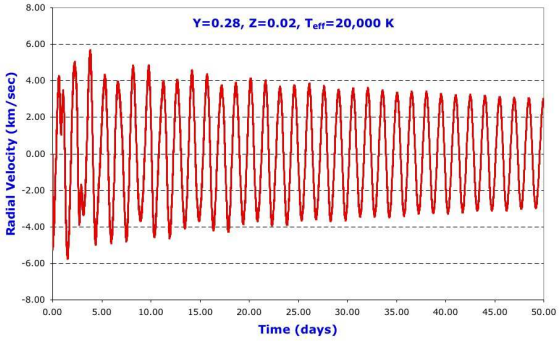

Fig. 16.— Radial velocity of the photosphere vs. time for the same model as in Figure 15, but with the T_{eff} changed to 20,000 K, while all other parameters are held constant. The pulsation amplitude decreases with the decrease in effective temperature.

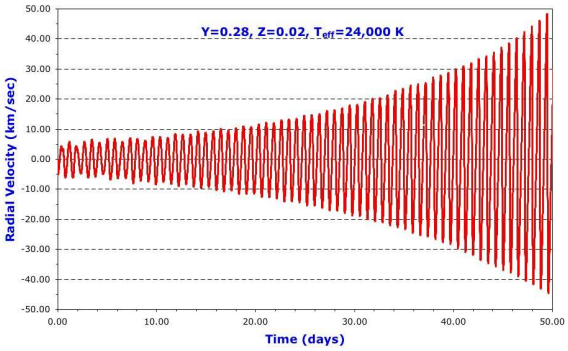

Fig. 17.— Radial velocity of the photosphere vs. time for the model from Figure 15 with the temperature increased to 24,000 K. The increase in effective temperature results in a growth in the pulsation amplitudes.

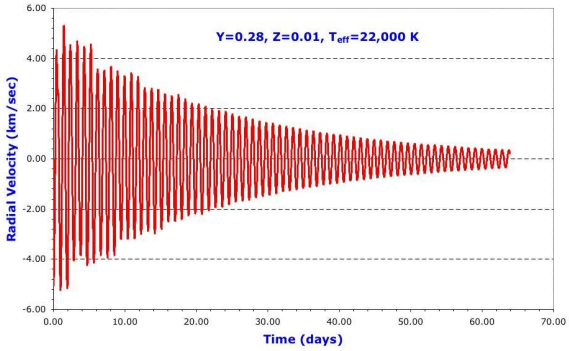

Fig. 18.— Radial velocity of the photosphere vs. time for the model from Figure 15, but with the metallicity changed to 0.01, and all other parameters held constant. The pulsation amplitude damps quickly when the Z abundance is decreased.

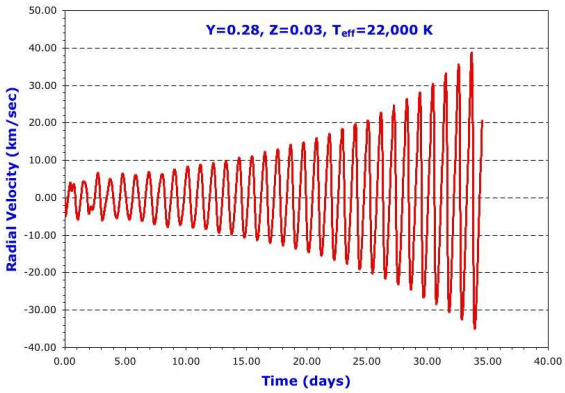

Fig. 19.— As for Figure 18, but with the metallicity increased to 0.03. In this case, the pulsation amplitudes grow rapidly.

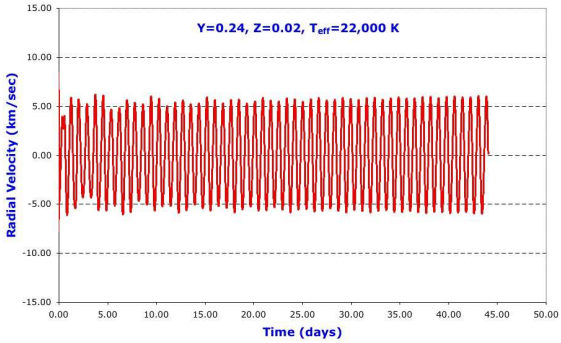

Fig. 20.— Radial velocity of the photosphere vs. time for the model from Figure 15 with the helium abundance (Y) decreased to 0.24. When Y is decreased in the envelope, the pulsation amplitude grows slowly, and the amplitude is smaller.

increase with increasing Z (increasing Fe) and decreasing Y (He) in envelope. For the metallicity dependence, this behavior is consistent with the results of Shiode et al. (2012).

In future work, we could explore the effects of different masses, overtones, zoning, and depth of the envelope models. We would also like to test predictions observationally. However, stars of this mass are relatively rare, and evolve through this evolution state (shell H-burning) relatively rapidly, so may be difficult to observe. In the longer lived main-sequence phase, these stars are nonradial pulsators, and rotating rapidly, whereas we have only considered radial and non-rotating models. It would be useful to extend these models to 2D to include the effects of rotation. Other improvements could include the ability to lose mass from the surface, allowing us to follow our models through an outburst and recovery.

4. Giant Eruptions

4.1. Giant eruptions and rebounds

As discussed by Humphreys et al. (1999), there is evidence for several of the most luminous LBVs (Eta Car, P Cyg, SN 1961v and V12 in NGC 2403) that have shown giant eruptions, that a giant eruption is followed by a 'bounce' or 'rebound' as evidenced by a smaller increase in luminosity, one or more decades later (Figure 22).

Eta Carinae has been observed during two giant eruptions: the Great eruption in the 1840s, and a lesser eruption in the 1890s. The Great Eruption lasted for around 20 years, and was accompanied by a brightening of about 2 bolometric magnitudes. Measurements of the nebula produced by this event, the Homunculus, indicate that this eruption ejected on the order of 10 $M_{\odot}$. The lesser eruption in the 1890s may have been a rebound from the Great Eruption, and ejected less mass, visible in the Little Homunculus; see Figure 23 outlining this scenario from Smith et al. (1998). There is also evidence for previous eruptions in Eta Car occurring about 200 years ago. And there is some evidence that the eruption cycle in Eta Car is related to the orbital period of a binary companion (Smith & Frew 2011).

A second galactic LBV, P Cyg, was observed during a giant eruption, first around 1600 and again around 1640. In this star, the eruptions are

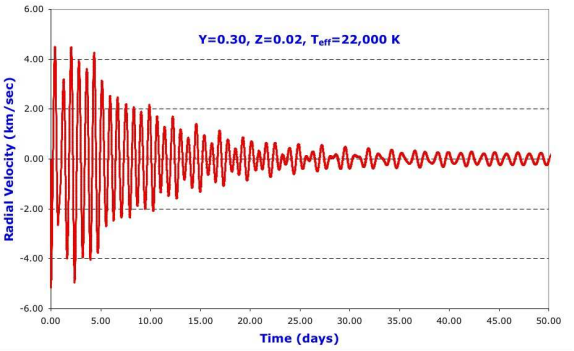

Fig. 21.— As for Figure 20, but with the helium abundance increased instead of decreased. The increase in helium abundance rapidly damps the pulsation amplitude.

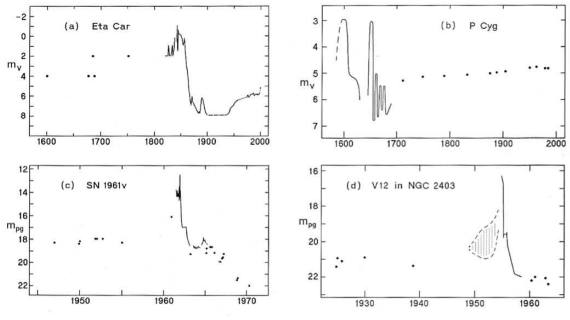

Fig. 22.— Light curves of four supernova impostors. a) Historical light curve of Eta Car. b) Historical light curve of P Cyg. c) Light curve of SN1961v. d) Light curve of V12, an extragalactic LBV. From Humphreys et al. (1999).

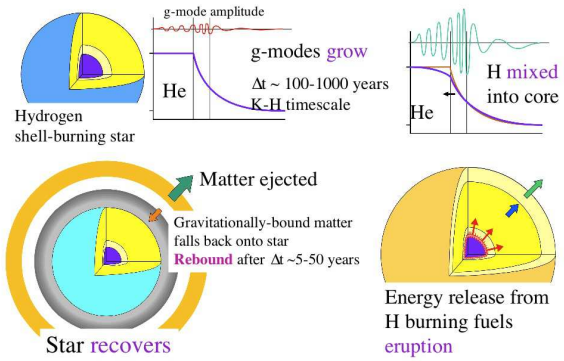

Fig. 24.— Suggested scenario for initiating giant eruptions by recurring nuclear event. The amplitude of gravity modes grows on a thermal timescale, mixing some hydrogen into the core. This triggers a burst of nuclear energy, which causes material to be ejected. This ejection is accompanied by a large increase in luminosity. After the eruption, some of the material settles back onto the star and the cycle begins again.

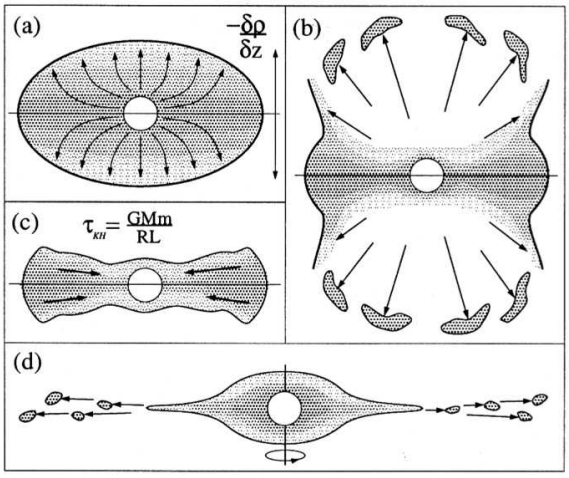

Fig. 23.— Proposed scenario for Eta Car from Smith et al. (1998). A pre-eruption rotating star has a vertical density gradient. In panel b, the Great Eruption ejects material from the poles of the star. Post eruption, the stellar envelope readjusts itself (panel c). During the 1890 eruption, material is ejected from the rapidly rotating envelope in the equatorial plane (panel d).

shorter, with a duration of about 6 years. Again, the eruptions were accompanied by an increase in bolometric magnitude. There is also evidence for previous eruptions between 900 and 2000 years ago.

The 'rebound' time between the greater and lesser eruption is expected to be the thermal, or Kelvin-Helmholtz timescale of the matter involved in the outburst.

The Kelvin-Helmoltz time is approximately

$$t_{K-H} \sim \frac{GM^2}{RL}, \qquad (13)$$

where G is Newton's gravitational constant, M is stellar mass, R is stellar radius, and L is stellar luminosity (see, e.g., Aerts, Christensen-Dalsgaard & Kurtz 2010, p. 26). We can use this formula to solve for the amount of mass above the core that must have participated in the eruption (ΔM), and is recovering from the eruption on this timescale.

If we convert to solar units and years, and break the mass up into M (total mass of the star) and ΔM (mass of the recovering layer), then we derive

$$\Delta M = 3.2 \times 10^{-8} \frac{RLt_{recov}}{M} \ \mathrm{M}_\odot. \qquad (14)$$

If we take the time between the greater and lesser eruption for Eta Carinae as t_{recov} ~30 years, and adopt for Eta Car M=80 $\mathrm{M}_\odot$, R=200 $\mathrm{R}_\odot$, L=5 $\times 10^6$ $\mathrm{L}_\odot$, then we find that the amount of

mass that must have participated in the eruption is $\Delta M = 12$ M$_\odot$.

This large amount of participating mass, as well as the large luminosity change of Eta Car during outburst, imply a very deep-seated mechanism for the outbursts. The result also implies that, for a given amount of mass that escapes, several times more mass settles back to near its initial configuration during the recovery.

Because of the low mass in the outer layers of these luminous stars (recall that 99.8% of the stellar mass lies within the inner several percent of the stellar radius), the origin of the giant eruptions ejecting tens of solar masses must originate deep in the core of star. Considering the behavior of stars exhibiting giant eruptions such as Eta Car and P Cyg, a mechanism for the giant eruptions must turn on relatively suddenly, and then, perhaps after a bounce/rebound, turn off for hundreds or even thousands of years. The mechanism must also generate additional energy, since large luminosity increases are seen during outbursts, and the mechanism needs to lift a large amount of mass out of a deep gravitational potential well.

4.2. Gravity-mode mixing

Here we outline a scenario that might produce the conditions described above, namely a mixing episode, perhaps initiated by gravity-mode oscillations, that mixes additional hydrogen inward to a region where it burns abruptly.

Gravity modes can be initiated by turbulent processes in the envelope (e.g., Stothers 2000; Samadi et al. 2010). For evolved stars, a dense spectrum of g modes is present with closely spaced nodes in a g-mode cavity formed at the edge of a burned-out core where there is a steep composition gradient (see, e.g., Guzik et al. 2000; Templeton 2000; Templeton et al. 2000, for examples based on shell hydrogen-burning δ Scuti stars). While g modes oscillate at periods near the dynamical timescale (days), they grow (or damp) in amplitude over the thermal or Kelvin-Helmholtz timescale ($\sim$100 years for Eta Car; $\sim$1000 years for P Cyg). The g-mode amplitudes could grow in the composition gradient region around the H-burning shell, and cause some hydrogen to mix into the H-exhausted core, producing a burst of nuclear energy and triggering an eruption, accompanied by a large luminosity increase and ejection of some mass. Gravitationally-bound material then settles back on to the star. The recovery time should be the Kelvin-Helmholtz timescale for the infalling material, 5-50 years, or the recovery times seen between major outbursts in Eta Car. The g modes are initiated again later to slowly grow in amplitude, restarting the cycle. This process is illustrated in Figure 24.

4.3. Additional possible mechanisms for initiating giant eruptions

Here we mention a few other mechanisms that may operate deep enough in the star and involve enough of the stellar mass to initiate giant eruptions, and should also be explored.

4.3.1. Secular/thermal instability

In standard pulsation analysis, such has been described above, the pulsation frequencies are found by perturbing a model in hydrostatic equilibrium. The resulting periods are on the order of the dynamical timescale of the star. However, an analysis could be done where the model is forced to be in hydrostatic equilibrium, but oscillations around thermal equilibrium, on the longer Kelvin-Helmholtz timescale are followed. The theory of secular stability and application to stellar structure and pulsations is reviewed by Hansen (1978). Pulsations arising from such secular or thermal instabilities (if found), may have the right periods and depths in the star to initiate the giant eruptions.

4.3.2. Epsilon mechanism

The epsilon mechanism is a pulsational instability arising from modulated nuclear energy generation in the cores of stars (Kippenhahn & Weigert 1990). The mechanism continues to be explored to explain pulsations in massive stars (e.g., Moravveji et al. 2011; Shiode et al. 2012) and in low-mass low metallicity stars (e.g., Sonoi & Shibahashi 2012). However, modes initiated by this mechanism may also be damped by turbulent viscosity or processes in the overlying stellar layers, and so far no variable stars classes have been been verified observationally with pulsations arising from this mechanism. Since this instability would originate deep in the core of an LBV star where nuclear

energy generation is occurring, it is in the right location to play a role in initiating a giant eruption.

4.3.3. Standing Accretion Shock Instability

The SASI (Standing Accretion Shock Instability) mechanism (see, e.g., Foglizzo 2008; Blondin et al. 2003; Scheck et al. 2008) has been suggested to assist in explosions in core-collapse supernova, and perhaps also explains the asymmetry of the ejecta. Accretion shocks occur not only in supernovae, but also in star formation and accreting compact objects. This instability does not necessarily require conditions present only in core-collapse supernovae, such as neutrino heating, but requires inflow and vorticity plus acoustic waves, and produces a nonradial l=1 oscillation that can grow in amplitude. The mechanism was even demonstrated in a scaled laboratory experiment using shallow water (Foglizzo 2012). Since for LBV stars a longer timescale is available for the instability to grow compared to the time after the post-bounce accretion phase of a supernova, perhaps this mechanism could also play a role in assisting the LBV giant eruptions.

4.3.4. Tidal effects from binary companions and rapid core rotation

The roles of tidal forces from binary companions and possible rapid core rotation in initiating LBV giant eruptions should also be investigated.

5. Future work and requirements

In this paper, we have only investigated in 1-dimension (1-D), for radial modes, in spherically symmetric, single, non-rotating models, some effects of helium, metallicity, effective temperature, and the luminosity/mass ratio on linear and nonlinear pulsations, and we have shown that taking into account the time-dependence of convection tin he hydrodynamic models allows the Eddington limit to be exceeded in the deeper envelope layers, and may initiate mass outflows.

There is utility in extending and improving these 1-D linear and nonlinear hydrodynamical models. We could refine zoning, try to improve the numerical stability by eliminating opacity table interpolation, continue running the models for longer times to look for possible mode changes, extend the parameter studies to additional masses, metallicities, and study the effect of the time-dependent convection parametrization.

However, other aspects of these problems seem more important for understanding LBVs, and require advances in modeling. It will be important to add an outflow boundary condition to the evolution and pulsation models to model the most massive stars that are not in hydrostatic equilibrium in their outermost layers. It may be important to numerical stability and keeping reasonable timesteps to use an adaptive grid code to rezone the envelope to adapt to the changes in radius during the pulsations. A means to remove and replenish mass in the envelope and follow mass loss is critical to predicting mass-loss rates or possible recovery from a mass-ejection episode. For this improvement, one may need to deal with opacity/EOS for low-density, non LTE effects, and improve radiation transport models.

In addition, not only radial, but also nonradial modes likely play a role, and so a nonlinear and nonradial pulsation code may be needed. Nonradial phenomena are evident in many LBV stars (Weis 2012) such as the bipolar nebula and 'skirt' in Eta Car.

Two-dimensional and three-dimensional codes may be required to model the effects of convection and convective overshoot, and model the time dependence of convection more realistically, deal with rapid and probably differential rotation, the tidal effects of possible binary companions, or investigate episodic mixing that might be produced by gravity modes or convective plumes.

The physics models and computational capabilities to handle these diverse phenomena are available in astrophysical codes being developed today, but perhaps not assembled to address specific aspects of LBV pulsation and mass outflow or interior instability problems in any one code (see, e.g., Guzik 2010, for a summary of results from some recent stellar interior hydrodynamics codes.). Some relevant capabilities were available in almost forgotten codes, such as the Bowen (1988) code developed to handle Mira mass loss, or the adaptive grid hydro code of Gehmeyr (1993) applied to RR Lyrae variable star pulsations. We hope that some of these tools can be adapted or resurrected and applied to the yet unexplained phenomena in LBV

stars.

Acknowlegements

The authors acknowledge Arthur N. Cox, Dale Ostlie, Kate Despain, Jay Onifer, Michael Soukup, Matthew Templeton, Benjamin Austin, Dean Pesnell, Brandon Peterson, and Siobahn Morgan, for calculating countless LBV models, attending and presenting at numerous conferences, and developing and providing the computational tools over the past 20 years. The authors thank many colleagues including Paul Bradley, Roberta Humphreys, Kris Davidson, S. Shore, H. Lamers, N. Smith, B. Wolf, A. Heger, A. Maeder, S. Owocki, N. Langer, and W. Glatzel for encouragement and important discussions. The authors also thank the anonymous referee who provided a thorough review of this paper with a short deadline despite its preliminary draft form when submitted. This work was performed for the U. S. Department of Energy by Los Alamos National Laboratory under Contract No. DE-AC52-06NA2-5396.

REFERENCES

Aerts, C., Christensen-Dalsgaard, J. & Kurtz, D.W. 2010, *Asterorseismology*, Springer Astronomy and Astrophysics Library.

Abolmasov, P. 2011, "Stochastic variability of luminous blue variables," *New Astronomy* 16, 421.

Alexander, D. & Ferguson, J. 1994, ApJ, 437, 875.

Alexander, D. & Ferguson, J. 1995, private communication.

*Austin, B.A., Guzik, J.A., Templeton, M.R., & Despain, K.M. 2004, in *Variable Stars in the Local Group*, eds. D.W. Kurtz & K. Pollard., ASP Conf. Ser. Vol. 310, p. 453.

Blondin, J.M., Mezzacappa, A., & DeMarino, C. 2003, ApJ, 584, 971.

Böhm-Vitense, E. 1958, Zs.F.Ap., 46, 108.

Bowen, G.H. 1988, ApJ, 329, 299.

Brunish, W. & Truran, J.W. 1982a, ApJ, 256, 247.

Brunish, W. & Truran, J.W. 1982b, ApJS49, 447.

Chiosi, C., & Maeder, A. 1986, ARA&A, 24, 329.

Clark, J.S., Castro, N., Garcia, M., Herrero, A., Najarro, F., Negueruela, I., Ritchie, B.W. & Smith, K.T. 2012, A&A, 541, A146.

Cox, A.N. 1983, in *Astrophysical Processes in Upper Main Sequence Stars*, 13th Advanced Course, Swiss Society of Astronomy and Astrophysics, ed. B. Hauck & A. Maeder.

Cox, A.N. 1990, "Pulsations of Delta Scuti Stars," in *Nonlinear Astrophysical Fluid Dynamics*, eds. J.R. Buchler & S.T. Gottesman, Annals of the NY Academy of Sciences, vol. 617, p. 54.

*Cox, A.N. & Despain, K.M. 2009, "Pulsation and Convection in Luminous Blue Variables," in *Stellar Pulsation: Challenges for Theory and Observation*, eds. J.A. Guzik & P.A. Bradley, Santa Fe, NM, AIP Conf. Proceedings 1170, p. 335.

*Cox, A.N & Guzik, J.A. 2008, "Pulsation and Convection in Luminous Blue Variable Stars," talk and proceedings for *Evolution and Pulsation of Massive Stars*, Liege, Belgium, July 7-10, 2008, CoAst,158, 259.

*Cox, A.N., Guzik, J.A., & Soukup, M.S. 1997, "Linear Pulsations of Strange Modes in LBVs," in *Luminous Blue Variables: Massive Stars in Transition*, October 6-11, 1996, Kona, Hawaii, eds. A. Nota & H.J.G.L.M. Lamers, ASP Conf. Ser. Vol. 120, pp. 133-137.

*Cox, A.N., Guzik, J.A., Soukup, M.S. & Morgan, S.M. 1995, "Theoretical Pulsations of Luminous Blue Variables," in *Proc. IAU Colloquium 155, Astrophysical Applications of Stellar Pulsation*, Cape Town, South Africa, Feb. 6-10, 1995, eds. R.S. Stobie & P. A. Whitelock, ASP Conf. Ser. Vol. 83, pp. 192-193.

*Cox, A.N., Guzik, J.A., Soukup, M.S. & Despain, K.M. 1998, "Pulsations and outbursts of luminous blue variables," in *A Half Century of Stellar Pulsation Interpretations*, eds. P. Bradley & J.A. Guzik, ASP Conf. Ser. 135, 302.

*Cox, A.N., Morgan, S.M., Soukup, M.S., & Guzik, J.A. 1993. "Predicted Nonradial Pulsations of Luminous Blue Variables," 183rd meeting of the American Astronomical Society,

Washington, D. C., January 11-15, 1994, abstract in Bulletin of the American Astronomical Society 25, 144.

Cox, A.N. & Ostlie, D.A. 1993, Ap&SS, 210, 311.

Cox, J.P. 1980, *Theory of Stellar Pulsation*, Princeton University Press, pp. 135-148.

Davidson, K. & Humphreys, R.M., eds. 2012, *Eta Carinae and the Supernova Impostors*, Springer Astrophysics and Space Sciences Library, vol. 384.

*Despain, K.M., Guzik, J.A., & Cox, A.N. 1998, "Nonlinear Pulsation Modeling of Luminous Blue Variables," in *A Half Century of Stellar Pulsation Interpretations*, ed. P.A. Bradley & J.A. Guzik, ASP Conference Series 135, p 307.

Dorfi, E.A. & Gautschy, A. 2000, "Where are the regularly pulsating massive stars?", ApJ, 545, 98.

Foglizzo, T. 2008, ASP, 385, 85.

Foglizzo, T., Masset, F., Guilet, J., & Durand, G. 2012, Phys. Rev. Letters, 108, 1103.

Gehmeyr, M. 1993, ApJ, 412, 341.

Glatzel, W. & Mehren, S. 1996, "Nonradial pulsations and stability of massive stars," MNRAS, 282, 1470.

Glatzel, W., Kiriakidis, M., Chernigovskij, S., & Fricke, K.J. 1999, "The nonlinear evolution of strange-mode instabilities,"MNRAS, 303, 116.

Glatzel, W. 1994, "On the origin of strange modes and the mechanism of related instabilities," MNRAS, 271, 66.

Glatzel, W. 1999, "Linear strange modes in massive stars," in *Proc. IAU Colloq. 169, Variable and Non-Spherical Winds in Luminous Hot Stars*, Heidelberg, Germany, June 15-19, 1998, eds. B. Wolf, O.Stahl, & A.W. Fullerton, Lecture Notes in Physics Vol. 523 (Springer, Berlin, 1999), pp. 345-352.

Grevesse, N. & Noels, A. 1993, Physica Scripta, Volume T, 47, 133

*Guzik, J.A. 2005, "Instability considerations for massive star eruptions," in *The Fate of the Most Massive Stars*, Grand Teton National Park, WY, May 23-28, 2004, eds. R. Humphreys & K. Stanek, ASP Conf. Ser. 332, p. 208.

Guzik, J.A. 2010,"Recent Advances in Modeling Stellar Interiors," Ap&SS, 336, 95.

Guzik, J.A. & Lovekin, C.C. 2012, "Pulsations and Hydrodynamics of Luminous Blue Variable Stars," Astronomical Review 7, 13.

*Guzik, J.A., Austin, B.A., Cox, A.N., & Despain, K.M. 2004, "The role of pulsations in mass loss from massive blue stars," in *Chemical Enrichment in the Early Universe*, Santa Fe, NM, ed. A. Heger, Los Alamos report LA-UR-05-0027.

*Guzik, J.A. & Austin, B.A. 2005, "Opacity Effects on the Pulsations of 20 Solar Mass Models," in *The Fate of the Most Massive Stars*, Grand Teton National Park, WY, May 23-28, 2004, eds. R. Humphreys & K. Stanek, ASP Conf. Ser. 332, 269.

*Guzik, J.A., & Austin, B.A. 2004, "Opacity Effects on the Pulsation of 20 $M_\odot$ Stellar Models", in *14th APS Topical Conference on Atomic Processes in Plasmas*, Santa Fe, NM, April 19-22, 2004.

Guzik, J.A., Bradley, P.A., & Templeton, M.A. 2000, ASPC 201, 247.

*Guzik, J.A., Cox, A.N., & Despain, K. 1999, "Pulsation-driven Outflows in Luminous Blue Variables," in *Eta Carinae at the Millenium*, July 20-23, 1998, Gallatin Gateway, Montana, eds. J. Morse, R. Humphreys, & A. Damineli, ASP Conf. Ser. 179, pp. 347-353.

*Guzik, J.A., Cox, A.N., & Despain, K.M. 2005, "Pulsation-Driven Mass Loss in Luminous Blue Variables," in *The Fate of the Most Massive Stars*, Grand Teton National Park, WY, May 23-28, 2004, eds. R. Humphreys & K. Stanek, ASP Conf. Ser. 332, p. 267.

*Guzik, J.A., Cox, A.N., & Despain, K. 1999, "Pulsation Hydrodynamics of Luminous Blue Variables and Pulsation-Driven Winds," in

Proc. IAU Colloq. 169, Variable and Non-Spherical Winds in Luminous Hot Stars, Heidelberg, Germany, June 15-19, 1998, eds. B. Wolf, O.Stahl, & A.W. Fullerton, Lecture Notes in Physics No. 523, (Springer, Berlin, 1999), pp. 337-344.

*Guzik, J.A., Cox, A.N., Despain, K.M., & Soukup, M.S. 1996, "A Nonlinear Study of Luminous Blue Variables and Possible Outbursts," in *Luminous Blue Variables: Massive Stars in Transition*, October 6-11, 1996, Kona, Hawaii, eds. A. Nota & H.J.G.L.M. Lamers, ASP Conf. Ser. 120, pp. 138-142.

Hansen, C.J. 1978, ARA&A, 16, 15.

Humphreys, R.M. & Davidson, K. 1994, PASP, 106, 1025.

Humphreys, R.M., Davidson, K., & Smith, N. 1999, PASP, 111, 1124.

Iben, I., Jr. 1963, ApJ, 138, 452.

Iben, I., Jr. 1965a, ApJ, 141, 993.

Iben, I. 1965b, ApJ, 142, 1447.

Iglesias, C.A. & Rogers, F.J 1996, ApJ, 464, 943.

Kippenhahn, R. & Weigert, A. 1990, *Stellar Structure and Evolution*, Springer Astronomy and Astrophysics Library, pp. 407-417.

Kotak, R. & Vink, J.S. 2006, A&A, 406, L5.

*Lovekin, C.C. & Guzik, J.A. 2011, "Pulsational Mass Loss in Luminous Blue Variables," in *Four Decades of Research on Massive Stars*, Saint-Michel-des-Saints, QC, July 11-15, 2011.

*Lovekin, C.C., & Guzik, J.A. 2011, "Pulsations in Hot Massive Stars," in *20th Stellar Pulsation Conference*, Granada, Spain, Sept. 5-9, 2011, Ap&SS, 31, 27.

Moravveji, E., Guinan, E.F., Moya, A., Williamson, M. & Fekel, F. 2011, 2011arXiv1109.6071M.

Najarro, F. 2001, in *P Cygni 2000: 400 Years of Progress*, eds. M. de Groot & C. Sterken. ASP Conference Series 233, 133.

Najarro, F., Hillier, D.J. & Stahl, O. 1997, A&A, 326, 1117.

Nieuwenhuijzen, H. & de Jager, C. 1990, ApJ, 464, 943.

*Onifer, A.J. & Guzik, J.A., 2007, "Hydrodynamic Modeling of Pulsation-Initiated Mass Loss in Luminous Blue Variables," B.A.A.S. 39, 871.

*Onifer, A.J. & Guzik, J.A. 2008, "Pulsation Initiated Mass Loss in Luminous Blue Variables: A Parameter Study," in *Massive Stars as Cosmic Engines, Proc. IAU Symp 250*, eds. F. Bresolin, P.A. Crowther & J. Puls, IAU 2008.

Ostlie, D.A. 1982, *Linear and Nonlinear Models of Mira Variable Stars*, Ph.D. Thesis, Iowa State University.

Ostlie, D.A. 1990, "Time Dependent Convection in Stellar Pulsation," in *Numerical Modelling of Nonlinear Stellar Pulsations Problems and Prospects*, ed. J. R. Buchler, (Kluwer Academic, Dordrecht), p. 89.

Pamyatnykh, A.A. 2002, Comm. Asteroseismology, 142, 10.

Pesnell, W.D. 1990, ApJ, 363, 227.

Puls, J., Vink, J.S. & Najarro, F. 2008, A&ARev 16, 209.

Rogers, F.J. & Iglesias, C.A. 1994, "Astrophysical Opacity," Science, 263, 50.

Saio, H., Baker, N.H., & Gautschy, A. 1998, "On the properties of strange modes," MNRAS, 294, 622.

Samadi, R., Belkacem, K., Goupil, M.J., Dupret, M.-A., Brun, A.S., & Noels, A. 2010, "Stochastic excitation of gravity modes in massive main-sequence stars," Ap&SS, 328, 253.

Scheck, L., Janka, H.-Th., Foglizzo, T. & Kifonidis, K. 2008, A&A, 477, 931.

Shaviv, N.J. 2000, ApJ, 532, L137.

Shiode, J.H., Quataert, E., & Arras, P. 2012, MNRAS, 3116.

Smith, N. 2010. in *Hot and Cool: Bridging Gaps in Massive Star Evolution*, eds. C. Leitherer, P. Bennett, P. Morris, & J. van Loon. ASP Conference Series 425, 63.

Smith, N. & Frew, D.J. 2011, MNRAS, 415, 2009.

Smith, N., Guzik, J.A., Lamers, H.J.G.L., Cassinelli, J., & Humphreys, R. 1998, in *Variable and Non-Spherical Winds in Luminous Hot Stars*, Heidelberg, Germany, June 15-19, 1998, eds. B. Wolf, O.Stahl, & A.W. Fullerton, Lecture Notes in Physics No. 523, (Springer, Berlin, 1999), pp. 249-250.

Smith, N., Li, Weidong, Silverman, J.M., Ganeshalingam, M., & Filippenko, A.V. 2011, MNRAS, 415, 773.

Smith, N. & Owocki, S.P. 2006, ApJ, 645, L45.

Sonoi, T. & Shibahashi, H. 2012, MNRAS, 422, 2642.

*Soukup, M.S., Cox, A.N., Guzik, J.A., & Morgan, S.M. 1994, "The Theoretical Instability Strip for Luminous Blue Variables," 184th meeting of the American Astronomical Society, Minneapolis, MN, May 29-June 2, 1994, Bulletin of the American Astronomical Society 26, 907.

Stahl, O., Jankovics, I., Kovacs, J., Wolf, B., Schmutz, W., Kaufer, A., Rivinius, T., Szeifert, T. 2001, A&A, 375, 54.

Stahl, O., et al. 2003, A&A, 400, 279.

Stellingwerf, R.F. 1975a, ApJ, 195, 441.

Stellingwerf, R.F. 1975b, ApJ, 199, 705.

Stothers, R.B. 2000, "Does turbulence in the iron convection zone cause the massive outbursts of Eta Carinae?", ApJ, 530, L103.

Templeton, M.R. 2000, *An Observational and Theoretical Study of High-amplitude delta Scuti Stars*, Ph.D. thesis, New Mexico State University, 127T.

Templeton, M.R., Bradley, P.A., & Guzik, J.A. 2000, ApJ, 528, 979.

Van Dyk, S.D. & Matheson, T. 2012, "The Supernova Impostors," in *Eta Carinae and the Supernova Impostors*, Springer Astrophysics and Space Science Library vol. 384, p. 275.

van Genderen, A.M., Steemers, W.J.G., Feldbrugge, P.T.M., Groot, M., Damen, E. & van den Boogaart, A.K. 1985, A&A, 153, 163.

van Genderen, A.M., Thé, P.S., Heemskerk, M., Heynderickx, D., van Kampen, E., Kraakman, H., Larsen, I., Remijn, L., Wanders, I. & van Weeren, N. 1990, A&A, 82, 189.

Vink, J. 2012, "Eta Carinae and the Luminous Blue Variables," in *Eta Carinae and the Supernova Impostors*, Springer Astrophysics and Space Science Library vol. 384, p. 221.

Vink, J.S. & de Koter, A. 2002, A&A, 393, 543.

Weis, K. 2012, "The Outer Ejecta," in *Eta Carinae and the Supernova Impostors*, Springer Astrophysics and Space Science Library vol. 384, p. 171.

Wolf., B., Kaufer, A., Rivinius, T., Stahl, O., Szeifert, T., Tubbesing, S. & Schmid, H.M. 2000, in *Thermal and Ionization Aspects of Flows from Hot Stars*, eds. H. Lamers & A. Sapar, ASP Conference Series 204, 43.

This 2-column preprint was prepared with the AAS LaTeX macros v5.2.